An Optimized Semidetailed Submechanism of Benzene Formation from Propargyl Recombination

Weiyong Tang,[†] Robert S. Tranter,[‡] and Kenneth Brezinsky*

Departments of Mechanical Engineering and Chemical Engineering, University of Illinois at Chicago, 842 W. Taylor St., M/C 251, Chicago, Illinois 60607

Received: May 26, 2005; In Final Form: November 11, 2005

The self-reaction of propargyl (C_3H_3) radicals has been widely suggested as one of the key routes forming benzene in a variety of aliphatic flames. Currently, in the majority of aromatic models, the $C_3H_3 + C_3H_3$ submechanism often contains one or two C_6H_6 isomers and a few global reaction steps, which do not adequately represent the actual recombination chemistry. Recent experimental and theoretical studies on the direct propargyl recombination and subsequent C_6H_6 isomerization have provided sufficient information to revisit and revise the $C_3H_3 + C_3H_3$ reaction submechanism. In the present work, a semidetailed kinetic model consisting of seven isomeric C_6H_6 species and 14 reaction steps was constructed based on the most recent potential energy surface for this system. The trial model was subjected to systemic optimization by use of a recently developed physically bounded Gauss−Newton (PGN) method against detailed species profiles of direct propargyl recombination and 1,5-hexadiyne (15HD) isomerization obtained from experiments at high temperatures in a shock tube and at low temperatures in a flow reactor, which were all measured at very high pressure (shock tube) or atmospheric (flow reactor) conditions. Predictions of the optimized model were in excellent agreement with all experimental measurements. The optimized $C_3H_3 + C_3H_3$ reaction subset was also tested for flame modeling. Two different aromatic chemistry models that incorporate benzene formation from propargyl radicals as a single step reaction were modified to include the complete submechanism for propargyl recombination. The updated models predict significant percentages of three isomeric species [2-ethynyl-1,3-butadiene (2E13BD), fulvene, and benzene] in premixed fuel-rich acetylene and ethylene flames, reflecting the observed flame structures.

Introduction

To minimize polycyclic aromatic hydrocarbons (PAH) and soot formation from combustion, it is necessary to understand benzene formation because the production of the first ring is believed to be the rate-limiting step in the formation of multiring compounds.[1−5] Despite its importance, the mechanism of benzene formation in combustion systems is still the subject of debate, with attention focusing mainly on two broad classes of reaction: (a) reactions of C_4 species with C_2 species and (b) reactions of C_3 species, in particular the self-reaction of the resonantly stabilized propargyl (C_3H_3) radical.[6−9]

Over the past few years, the self-reaction of propargyl radicals, R0,

$$C_3H_3 + C_3H_3 \rightarrow \text{Products} \qquad \text{(R0)}$$

has gained increasing attention because flame modeling studies indicate that R0 is the predominant route, forming benzene under various combustion conditions.[9−15] As a particular example to illustrate how important this route is, the predicted peak mole fraction of benzene is reduced significantly to 7.1×10^{-6} from 3.5×10^{-5} in a fuel-rich premixed ethylene/oxygen/argon flame ($\phi = 1.9$, 50.0% argon, $v = 62.5$ cm^{-1} s^{-1}, 20 Torr) if the propargyl recombination route is excluded from the kinetic model of Richter and Howard.[9]

Currently, in the majority of aromatic models, the submechanism of $C_3H_3 + C_3H_3$ is essentially constructed from the results of Melius and co-workers, obtained over one decade ago,[16,17] which do not include some recently discovered reaction pathways for benzene formation at relatively low temperatures. Instead, the current $C_3H_3 + C_3H_3$ submechanism often consists of only one or two C_6H_6 species, benzene and fulvene, and a few global reaction steps.[9−13] Such a representation is too simple to reflect the complexity of the $C_3H_3 + C_3H_3$ reaction and may potentially fail to model accurately the formation and consumption of benzene and the subsequent aromatic-ring growth. Consequently, it is reasonable to update the $C_3H_3 + C_3H_3$ submechanism with one based on the recent experimental and theoretical work on the propargyl self-reaction, which is briefly outlined below.

The overall recombination rate constant, k_0, has been experimentally determined by a number of real-time measurements, and the agreement is within 1 order of magnitude over a wide temperature and pressure range.[18] Of equal importance, the isomeric product nature of propargyl recombination has also been revealed in several experimental studies[18−23] that have permitted reaction pathways to be examined in detail. In addition, a recent high-pressure shock tube study of propargyl recombination has yielded branching ratios for the three entrance channels.[18]

In a recent theoretical investigation, Miller and Klippenstein [24] refined an earlier treatment of Melius et al.[16,17] and included a new reaction path that connects 1,2,4,5-hexatetraene (1245HT) to *cis*-1,3-hexadiene-5-yne (13HD5Y), which then goes on to

* Corresponding author. E-mail: kenbrez@uic.edu.
[†] Current address: Gamma Technologies Inc., 601 Oakmont Ln., Westmont, IL, 60559.
[‡] Current address: Chemistry Division, Argonne National Laboratory, Argonne, IL 60439.

10.1021/jp052797s CCC: $33.50
Published on Web 01/25/2006

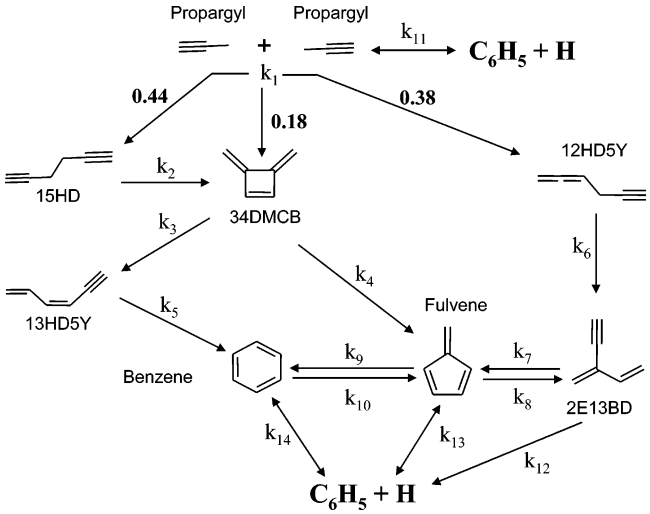

Figure 1. A semidetailed kinetic model of propargyl recombination and subsequent C_6H_6 isomerization. 15HD, 1,5-hexadiyne; 1245HT, 1,2,4,5-hexatetraene; 12HD5Y, 1,2-hexadiene-5-yne; 34DMCB, 3,4-dimethylenecyclobutene; 13HD5Y, 1,3-hexadiene-5-yne; 2E13BD, 2-ethynyl-1,3-butadiene.

benzene without passing through fulvene (see Figure 1 for structures). Such an alternate route to benzene appears warranted based on earlier experimental studies (see ref 30 for a detailed discussion). For benzene formation, the route via 13HD5Y is dominant at low temperatures and provides a lower temperature route to benzene, consistent with experimental data of 15HD isomerization, than can be achieved by isomerization of fulvene. Despite its potential importance, the 13HD5Y to benzene route, to the best of our knowledge, has not yet been included into detailed aromatic chemistry models.

Miller and Klippenstein also demonstrated that multiple C_6H_6 species lie on the $C_3H_3 + C_3H_3$ potential energy surface, some of which can be stabilized by collision, in competition with chemically activated isomerization. A considerable percentage of these C_6H_6 species have even been observed in premixed acetylene and ethylene flames by Westmoreland and co-workers.[25−27] Similarly, a rich variety of C_6H_6 species, including high mole fractions of 2E13BD, fulvene, and benzene, have been observed in a recent high-pressure shock tube (HPST) study of propargyl recombination.[18] These three isomers, 2E13BD, fulvene, and benzene, are capable of being stabilized at combustion temperatures (~1500 K).[24] Hence, theory strongly indicates that, in order to accurately predict benzene formation in combustion, it is necessary to account for multiple C_6H_6 species in flames, which cannot be done by the conventional $C_3H_3 + C_3H_3$ submechanism because normally it contains only fulvene and benzene as the isomeric products.

The goal of the present work is, on the basis of the new experimental and theoretical understanding of the $C_3H_3 + C_3H_3$ reaction described above, to develop a compact submechanism for propargyl recombination that can be incorporated into combustion models and provide predictions for the multiple C_6H_6 species involved in the formation of benzene. The methodology adopted in developing this model is novel and makes use of a recently developed numerical technique, the physically bounded Gauss−Newton (PGN) method,[28,29] to extract rate coefficients from the experimental data available in the literature. This method computes rate parameters numerically and, consequently, avoids having to extract phenomenological rate coefficients from the complex reaction network involved in the $C_3H_3 + C_3H_3$ potential energy surface by ab initio/RRKM−Master equation techniques.[24]

TABLE 1: Arrhenius Rate Parameters of Reactions in the Semidetailed Simplified Model of the $C_3H_3 + C_3H_3$ Reaction [$k = AT^b \exp(-E_a/RT)$][a]

	reaction	A	b	E_a	ref
1	$C_3H_3 + C_3H_3 \rightarrow$ 0.44 15HD + 0.18 34DMCB + 0.38 12HD5Y	1.00×10^{13}	0	0	36 18
2	15HD → 34DMCB	6.50×10^{10}	0	33 360	30
3	34DMCB → 13HD5Y	4.10×10^{12}	0	50 530	p.w.
4	34DMCB → fulvene	1.44×10^{13}	0	51 150	p.w.
5	13HD5Y → benzene	3.78×10^{12}	0	48 810	p.w.
6	12HD5Y → 2E13BD	2.75×10^{10}	0	34 960	18
7	2E13BD → fulvene	6.61×10^{12}	0	58 360	p.w.
8	fulvene → 2E13BD	9.12×10^{15}	0	82 700	p.w.
9	fulvene → benzene	9.89×10^{14}	0	70 470	p.w.
10	benzene → fulvene	5.53×10^{18}	0	100 400	p.w.
11	$C_3H_3 + C_3H_3 \leftrightarrow C_6H_5 + H$	3.67×10^{26}	−3.879	28 963	24
12	2E13BD → $C_6H_5 + H$	3.09×10^{43}	−7.928	118 650	24
13	fulvene ↔ $C_6H_5 + H$	8.51×10^{24}	−2.505	113 330	24
14	benzene ↔ $C_6H_5 + H$	5.50×10^{38}	−6.178	132 000	24

[a] Note: *A* units mol cm sec K, E_a units cal/mol. 15HD, 1,5-hexadiyne; 1245HT, 1,2,4,5-hexatetraene; 12HD5Y, 1,2-hexadiene-5-yne; 34DMCB, 3,4-dimethylenecyclobutene; 13HD5Y, 1,3-hexadiene-5-yne; 2E13BD, 2-ethynyl-1,3-butadiene.

In the PGN method, rate parameters for a trial kinetic model are obtained through systematic optimization against reliable detailed species profiles from, in this case, both shock tube[18,30] and flow reactor[31] studies of direct propargyl recombination and 15HD isomerization over a wide temperature range at high-pressure conditions. The remainder of this paper discusses the development of an optimized compact $C_3H_3 + C_3H_3$ model by use of the PGN method and the application of the model in simulating flame data when the compact model is used in place of the one or two global reactions for propargyl recombination that are typically used.

Approach

1. Trial Model Construction. The trial (unoptimized) reaction model consists of 14 reactions and seven C_6H_6 isomers, Figure 1 and Table 1, which was constructed based on the recent experimental and theoretical studies of direct propargyl recombination and subsequent C_6H_6 isomerizations.[18,24,30,31]

The current treatment of a reaction system that contains many chemically activated individual steps with a pressure-independent set of thermal isomerization reactions is only an approximation that has been developed through mathematical parametrization. In the present work, the intrinsically pressure-dependent $C_3H_3 + C_3H_3$ system was treated as a two-step process: (1) the entry channels via various head/tail recombinations forming three linear C_6H_6 isomers (15HD, 1245HT, and 12HD5Y) and (2) the subsequent isomerizations of these chemical-activated complexes forming different C_6H_6 compounds. The use of 34DMCB as a surrogate for the 1245HT entrance channel is based on an earlier shock tube/GC-FID study of propargyl recombination that demonstrated that 1245HT is efficiently and predominantly converted to 34DMCB.[18] The experimentally determined entrance branching ratios were 44% 15HD, 38% 12HD5Y, and 18% 34DMCB, respectively. No significant temperature and pressure dependence of the branching ratios was observed in the shock tube study by using propargyl iodide as the radical precursor. At high temperatures, the $C_3H_3 + C_3H_3$ reaction can dissociate to form phenyl + H via a sequence of elementary steps,[24] which, for convenience, were lumped into one step as R11 in Figure 1. In the current work, the dissociation channel R11 was included in the trial

model, even though previous shock tube/H atoms ARAS work by Scherer et al. [21] revealed that the dissociation channel was insignificant (representing less than 10% of the overall recombination rate from 1100 to 2100 K at 1.5−2.2 bar). The initially formed products 15HD, 34DMCB, and 12HD5Y can be stabilized at moderate temperatures by collision with the bath gas or can isomerize at higher temperatures to various C_6H_6 species, including 13HD5Y, 2E13BD, fulvene, and benzene via reactions R2−R10 in Figure 1. When the temperature is high enough, thermal dissociation of C_6H_6 isomers to phenyl radicals and hydrogen atoms occurs,[24] reactions R12−R14.

To model benzene formation accurately, an adequate description of 13HD5Y formation and destruction is necessary because it is the key intermediate in the low-temperature route to benzene.[24,30] Both *cis*- and *trans*-13HD5Y were observed in the same temperature range with roughly the same yields in shock tube studies of 15HD isomerization and direct propargyl recombination.[18,30] Two theoretical studies have been conducted on the energetics and kinetics of 13HD5Y. Both works distinguished two rotamers of 13HD5Y but showed considerable discrepancies. The calculations using a combination of QCISD-(T) and density functional (B3LYP) methods by Miller and Klippenstein generated the same ZPE (zero-point energy) for the two structures and obtained a tight transition state (TS) that is 49 kcal/mol higher than that of the rotamers[24] for the interconversion of the *cis*- and *trans*- forms. However, in a more recent work conducted at G2M level by Kislov and coworkers,[32] the TS has the same energy as that of the *cis*- and thus is much easier to cross. In addition, the Kislov work indicated the *trans*- rotamer is 3.9 kcal/mol below the *cis*-. Our preliminary modeling showed that the *trans*- rotamer mole fraction was greatly underpredicted if a 49 kcal/mol energy barrier was applied, while being enormously overpredicted if the barrierless TS was adopted. In neither case could benzene be well predicted. Consequently, in the present study, the two rotamers were lumped, with an assumption that the rate parameters of R3 (producing 13HD5Y) and R5 (consuming 13HD5Y) will be automatically adjusted by the optimization to account for the interconversion between the two rotamers.

Reliable thermodynamic data for most of the C_6H_6 isomers are not available in the literature, which is potentially significant if the reactions in the compact model are treated as reversible and the back rate coefficient is calculated from the equilibrium constant. One advantage of the current PGN method for extracting rate parameters for the optimized model is that, by treating the reactions as unidirectional, the optimization technique implicitly accounts for the back reaction by the way the model results are adjusted to fit the experimental data. Thus, the need for high-quality thermochemical data to calculate equilibrium constants is avoided and the resulting optimized compact model can be easily inserted into existing models. In this regard, the present result will not be affected by the thermodynamic findings in ref 24. A further consideration is that the thermodynamic properties of the various C_6H_6 isomers need to be known so that the effect of heats of reaction at the reaction temperature can be calculated during simulations that use the model. However, in contrast to the calculation of back reaction rates, it is not necessary to have very accurate thermochemistry for computing enthalpy changes due to C_6H_6 reactions because the concentrations of these species are typically very small compared to the bulk reaction mixture. Thus, for this purpose, it is sufficiently accurate to use the thermodynamic properties for benzene,[33] fulvene,[34] and 15HD[35] from the literature and use the 15HD value for the other linear C_6H_6 species and benzene for 34DMCB.

Additional starting data for the trial model were obtained as follows. The overall recombination rate constant, k_1, was taken from the experimental value of Fernandes et al.,[36] measured at 994−1440 K and 0.6−1.0 bar by using shock tube/UV absorption. Rate parameters for dissociation reactions, R11−R14, were taken from the time-dependent solutions of RRKM-based master equations calculated at 10 atm.[24] Rate constant expressions for the isomerization reactions 15HD → 34DMCB, R2, and 12HD5Y → 2E13BD, R6, were previously experimentally determined in the high-pressure shock tube[18,30] and hence were used unchanged in this work. The Arrhenius rate parameters, including both preexponential factor and activation energy, of the remaining seven isomerization reactions (k_3−k_5 and k_7−k_{10}), were set as active parameters and optimized systematically against measured species profiles, detailed later. The challenge associated with the trial model construction is the lack of reliable rate constant information, in contrast to other work also aimed at obtaining an optimized kinetic model where extensive rate constant recommendations are available for elementary reaction of interest.[37] Classical transition-state theory can provide order-of-magnitude estimates of preexponential factors and was applied to provide initial guesses in the current study. Critical barrier heights were approximated as activation energies subject to optimization.

2. Optimization and Computational Procedure. The determination of rate parameters in the trial model in Figure 1 from experimentally measured data can be mathematically expressed as a nonlinear dynamic minimization problem in system 1:

$$\min_{P} F(P) = \sum_{i=1}^{m} \left(\frac{y_i^{\exp} - y_i^{\mathrm{cal}}}{y_i^{\exp}} \right)^2 \tag{1}$$

subject to

$$\frac{\mathrm{d}y^{\mathrm{cal}}}{\mathrm{d}t} = f(y^{\mathrm{cal}}, P), \qquad y^{\mathrm{cal}}(t_0) = y^0 \tag{1-a}$$

where m refers to the total number of observed discrete experimental data points. The solution is the set of unknown parameters, P, that leads to the smallest error between the experimentally observed concentrations, $y^{\exp}$, and the model predictions, y^{cal}.

To solve the optimization problem, a recently developed novel deterministic method, the physically bounded Gauss−Newton (PGN) approach,[28,29] was employed. With respect to the utilization of sensitivity information, the "automatic" optimization scheme for the reaction rate parameters identification is similar to the solution-mapping approach of refs 37−39. But the PGN approach solves directly the dynamic optimization problem without the algebraic representation (i.e., solution mapping[39]) of the cost function by proceeding the Gauss−Newton update with physical trust region bounding.

The detailed mathematical formulation and validation of the PGN approach has been fully described elsewhere.[29] Briefly, an explicit map between the concentrations and kinetic parameter variations is first generated by using the first-order sensitivity information. This map constitutes a first-order approximation of the true response surface, relating each species trajectory to kinetic parameter perturbations. At every iteration step, a Gauss−Newton update equation is solved by the Broyden−Fletcher−Goldfarb−Shanno (BFGS) algorithm by

using the line search method to find the optimal perturbation that minimizes the residual error between experiment and prediction.[29] To avoid the departure of variables outside their definition space, a physical approach bounding the variable updates, detailed later, is enforced while providing the largest step length to facilitate convergence.

The optimization scheme described above was implemented with Chemkin-II[33] and Senkin.[41] In our previous work,[29] the PGN method was successfully tested on recovering preexponential factors on both linear and nonlinear reaction networks, some of which have a similar dimensionality to that in the present work. Here, we went a step further and extended its application to both activation energies and preexponential factors as follows. For the algorithm to find solutions, it requires sensitivity information with respect to the parameters that need to be optimized. In this case, the sensitivity of the experimental mole fractions with respect to both preexponential factors, *A*, and activation energy, *E*, are required for the PGN method to be successful. Senkin[41] computes only the sensitivity of mass fractions with respect to *A* through a perturbation factor, α, via eq 2. In the current work, it was necessary to modify Senkin so that the sensitivity of mass fraction with respect to *E* was also obtained. To achieve this, eq 3 was incorporated to compute the sensitivity information of mass fraction with respect to *E*. Although the sensitivities with respect to *A* and *E* were treated in a similar way, such that *E* is more strongly influential than *A*, it does not affect the solution of the Gauss−Newton update equation. That means the BFGS line search will provide a suitable length to update each parameter, minimizing the discrepancy between experiment and prediction.

$$k(\alpha A) = \alpha A T^b e^{-E/RT} = \alpha k(A) \tag{2}$$

$$\begin{aligned} k(\alpha E) &= A T^b e^{-\alpha E/RT} = A T^b (e^{-E/RT})^\alpha \\ &= (A T^b e^{-E/RT})^\alpha (A T^b)^{1-\alpha} = (A T^b)^{1-\alpha} k^\alpha(E) \end{aligned} \tag{3}$$

The sensitivity information of mole fraction with respect to *A* and *E* is computed through mass fraction sensitivity information by use of eq 4

$$\frac{\partial x_i}{\partial \alpha_j} = \frac{\bar{w}}{w_i}\left(\frac{\partial x_i}{\partial \alpha_j} - y_i \bar{w} \sum_{i=1}^{K} \frac{\partial y_i/\partial \alpha_j}{w_i}\right) \tag{4}$$

where w_i is the molecular weight for the *i*th species and $\bar{w}$ is the average molecular weight:

$$\bar{w} = \frac{1}{\sum_{i=1}^{K} y_i/w_i} \tag{5}$$

Having constructed a model for optimization, the initial parameters in the model need to be estimated. The initial parameter guess is of great importance. Experimental values, if known, can be used. Alternatively, classical transition-state theory (TST) can provide order-of-magnitude estimates of preexponential factors and the activation energy can be estimated from heats of formation. One potential problem from making such initial estimates is that the optimal solution is usually far away from the initial guess, which in combination with the inherent errors in the experimental data poses a great challenge to any deterministic methods, including the PGN approach, because of their inherent locality. Consequently, during the course of optimization, a trial-and-error model adjustment with a previously obtained solution was also applied to choose a new starting point to ensure that an "optimal" rate parameter set was achieved in a multidimension space.

To proceed with the PGN optimization in each run, the uncertainties of the estimated individual parameters need to be specified. More realistic bounds of the optimization parameters can be determined by studying the consistency of collaborative dataset on the combinational basis of solution mapping and robust control theory, which was demonstrated by Frenklach and co-workers.[40] In the current study, we did not transfer the uncertainties of the "raw" experimental data into the model prediction directly. Instead, we focused on the parametrization of the parameter uncertainty region. Here, the *A* factors were preassigned with a value of 10^{13}, if experimental recommendations are not available (R5, R7, R8, and R10), and allowed to vary in an uncertainty region of $10^{12}-10^{14}$. The variation range of activation energy was set to be (E_0/1.1, E_0*1.1), where E_0 was an estimate. If the optimized value lies on the bounds and the agreement between experiments and predictions is not acceptable, we adjusted the bounding range accordingly in the next optimization run.

The experimental data for the kinetic model development were taken from C_3H_3 recombination[18] and subsequent 15HD isomerization[30,31] experiments that represent the recombination chemistry. The kinetic model in Table 1 was used, without any alteration, in the 15HD simulations simply by setting the reagent mole fraction to be $[15HD]_0 = 1.0$. When simulating shock tube study of direct propargyl recombination, the dissociation of propargyl iodide,[18] R15, and the recombination of iodide atoms,[42] R16, were added because experiments were performed with propargyl iodide (C_3H_3I) as the radical (C_3H_3) precursor.

$$C_3H_3I \rightarrow C_3H_3 + I \qquad k_{15} = 10^{8.12} \times \exp(-20.9\ \text{K cal}/RT)\ \text{s}^{-1} \tag{R15}$$

$$I + I \rightarrow I_2 \qquad k_{16} = 10^{13.00}\ \text{cm}^6/(\text{mol}^2\cdot\text{s}) \tag{R16}$$

When the optimized subset was incorporated into a detailed aromatic model, a premixed flame structure was calculated by using Premix, an application program of the Chemkin collection,[43] considering thermal diffusion and multicomponent transport. The transport coefficients of C_6H_6 isomers, except fulvene and benzene, which are usually contained in a flame model, were calculated by using empirical formulas [44] from their Lennard−Jones parameters that were estimated by Joback's group contribution method.[45]

Results and Discussion

1. Model Validation. The trial model was subjected to systematic optimization and rigorous validation against reliable detailed species profiles of (a) the recombination of propargyl radicals at 25 bar from 720 to 1350 K by Tang et al.[18] (shock tube, seven species profiles), (b) the 1,5-hexadiyne isomerization at 25 bar from 800 to 1360 K by Tranter et al.[30] (shock tube, six species profiles), and (c) the low-temperature atmospheric 1,5-hexadiyne isomerization at 250−580 °C by Stein et al.[31] (flow reactor, four species profiles). Species profiles in shock tube studies at higher pressures were also obtained but were not included in the optimization because it was found that pressure influences on product distributions are barely discernible.[18,30] The resulting optimized reaction model of $C_3H_3 + C_3H_3$ subset, Table 1, along with its thermochemistry and transport property are available in the Supporting Information.

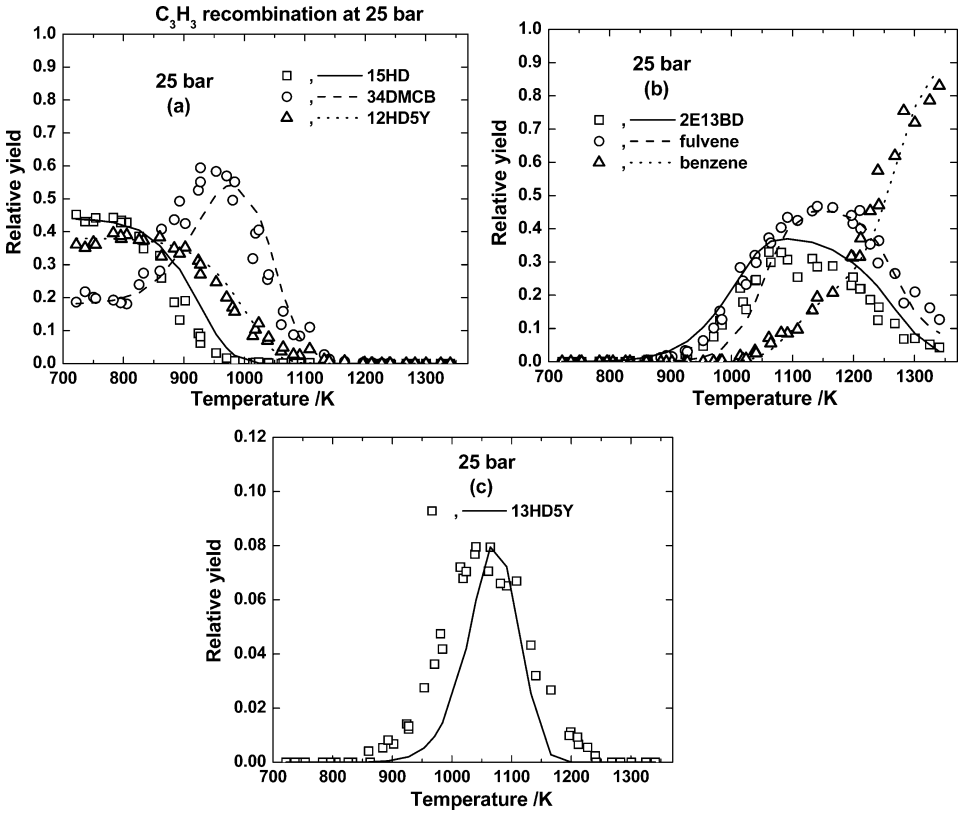

Figure 2. Observed (symbols, ref 18) and predicted (lines) isomeric C_6H_6 products profiles in propargyl recombination by using propargyl iodide (C_3H_3I) as the radical precursor at 25 bar ($[C_3H_3I]_0 = 45-65$ ppm).

By using the PGN approach, optimal rate parameters of the seven isomerization reactions (k_3-k_5 and k_7-k_{10}) were determined. Their Arrhenius parameter values (A and E) are displayed in Table 1. The optimized $C_3H_3 + C_3H_3$ subset predicts experimental species concentrations well in all shock tube studies, as shown in Figures 2 and 3. Note particularly that the peak concentrations of all the stable species are predicted to within a 10% deviation, and better in most cases. Generally speaking, the model is able to simulate perfectly the earlier (more active) product wells of the $C_3H_3 + C_3H_3$ reaction, in particular 15HD, 34DMCB, 12HD5Y (Figures 2a and 3a), and 13HD5Y (Figures 2c and 3c), where the temperatures of starting decay or build up were accurately predicted. However, the model showed a slight deficiency in predicting later (more stable) product wells of 2E13BD (Figure 3c), fulvene, and benzene (Figure 3b), the implication of this will be discussed later. The only significant discrepancy occurs in predicting 2E13BD in the shock tube study of 1,5-hexadiyne, Figure 3c, where the prediction are off by more than 50 K. Nevertheless, the model predicts a peak value that is consistent with that observed.

The sensitivity of optimized rate parameters on model performance was investigated. It was found through the optimization that rate parameters of the isomerization reactions (R3−R5) between earlier wells were much easier to determine than the later ones (R7−R10). In general, the overall predictive capability of the resulting model is much more sensitive to the parameters ranges of R7−R10 than to that of R3−R5. Clearly, there is a need for more experimental information about reactions R7−R10 in order to reduce the uncertainties of the current optimization. A detailed sensitivity analysis has been performed with 34DMCB and benzene as two examples as shown in Figures 4 and 5, respectively. In the figures, sensitivity spectra were evaluated at the specific reaction conditions of each data set. Note the data set were plotted according to the test temperatures of the discrete experiments. Figure 4 shows clearly that the most important reactions affecting the 34DMCB prediction are R3 and R4, with sensitivity spectra occurring in the temperature range of 900−1050 K. In comparison, as indicated in Figure 5, at higher temperatures $T > 1050$ K, the benzene profile is largely affected by A values of R7, R9 and R10, in addition to R3 and R4, which strongly suggests the necessity of studying the isomerization kinetics of 2E13BD and fulvene.

The optimized subset, without any modification, has the capability to predict product yields extremely well, Figure 6, in the low temperature (250−580 °C) atmospheric 15HD isomerization study by Stein and co-workers[31] using a flow reactor, a reactor that is systematically different from the shock tube apparatus. Such a demonstrated predictive capability for experimental measurements in both reactor types implies that the model contains the reactions of importance and captures the true chemistry of propargyl recombination. Additionally, the proposed model predicts a small amount of 13HD5Y in the temperature range of 410−530 °C, which was not experimentally observed by Stein et al., with a peak relative yield of about 10% at 480 °C that is in very good agreement with the theoretical calculation (Figure 5 in ref 24) by Miller and Klippenstein.

Previously Miller and Klippenstein performed RRKM-based multiwell multichannel master equation calculations over the whole $C_3H_3 + C_3H_3$ potential that consists of 104 elementary reaction steps.[24] The kinetic solutions obtained by using an ordinary differential equation (ODE) integrator to solve energy-grained population equations gave good predictions of Stein et al.'s flow reaction reactor pyrolysis of 15HD. On the basis of their time dependent solutions, Miller and Klippenstein[24] proposed a simplified 10-step model of the $C_3H_3 + C_3H_3$ recombination for flame modeling by lumping all products into

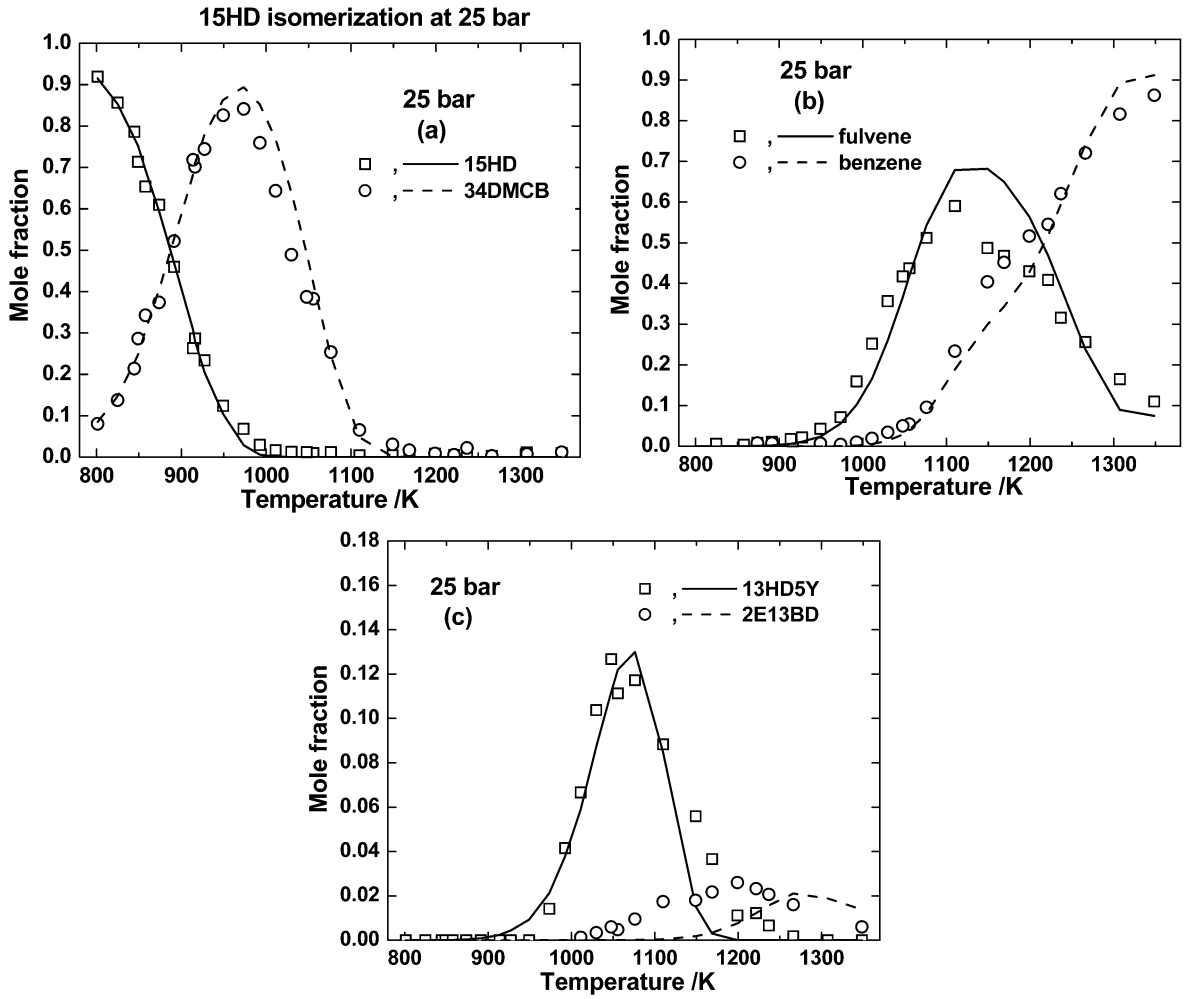

Figure 3. Observed (symbols, ref 30) and predicted (lines) isomeric C_6H_6 species profiles in 15HD isomerization at 25 bar ($[15HD]_0 = 42$ ppm).

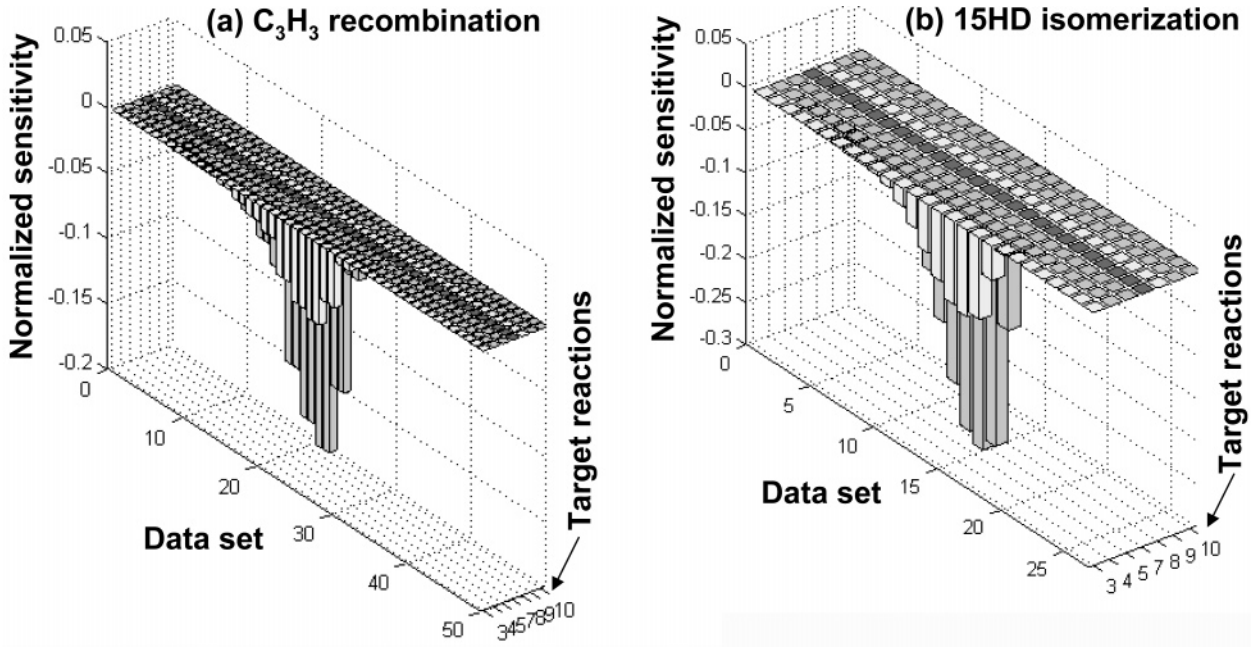

Figure 4. Sensitivity spectra of 34DMCB with respect to optimized individual preexponential factors in (a) the propargyl recombination study and (b) the 15HD isomerization study. Note: the data set were ranked according to the test temperatures of the discrete experiments. Detailed experimental information can be found in refs 18 and 30, respectively.

four different channels that contain only three C_6H_6 isomers, fulvene, 2E13BD, and benzene. No detailed information regarding the lumping process and no validation of the resultant compact model against experiment were reported. Despite the potential uncertainty, the 10-step model has recently been incorporated into a detailed flame mode by Law et al.[27]

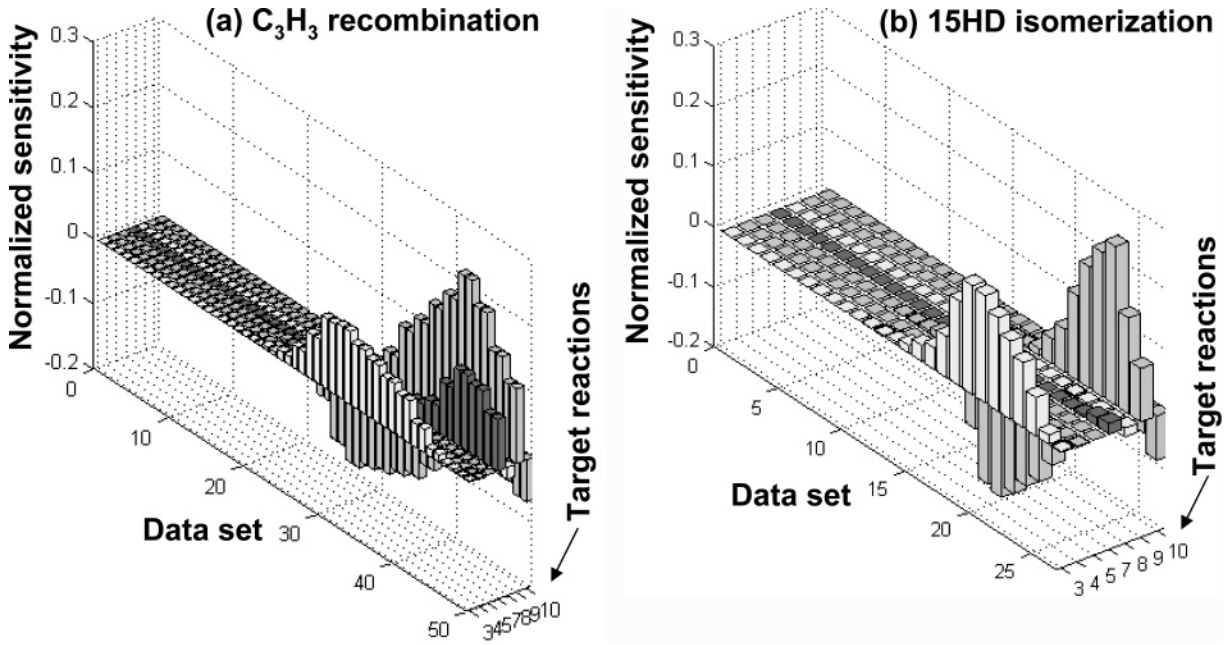

Figure 5. Sensitivity spectra of benzene with respect to optimized individual preexponential factors in (a) the propargyl recombination study and (b) the 15HD isomerization study. Note: the data set were ranked according to the test temperatures of the discrete experiments. Detailed experimental information can be found in refs 18 and 30, respectively.

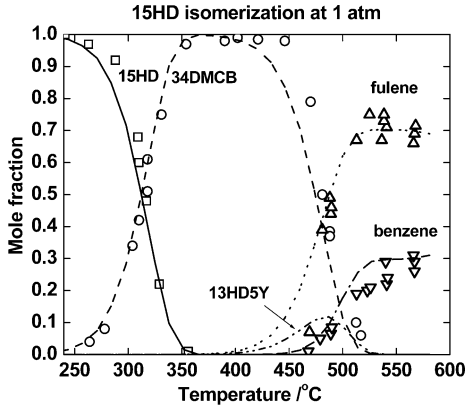

Figure 6. Observed (symbols, ref 31) and predicted (lines) isomeric C_6H_6 species profiles in 15HD isomerization at atmospheric pressure. 13HD5Y is predicted but was not detected.

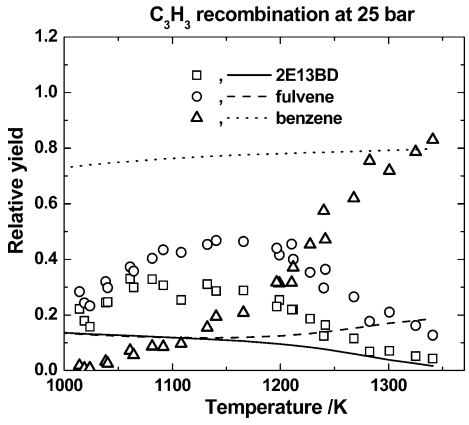

Figure 7. Predictive capability of a lumped 10-step model of the $C_3H_3 + C_3H_3$ reaction (ref 24). Symbols: experimental measurements (ref 18); lines: model predications.

Unfortunately, as clearly shown in Figure 7, the lumped 10-step model is not able to accurately simulate the recently obtained HPST experimental data of propargyl recombination. Note that, different from Figure 2b, Figure 7 only displays the comparison of the Miller and Klippenstein model predictions with experimental data in the higher temperature range, the range the model aims at, albeit the same data were used in these two figures. More comparisons with the theoretical approach on pressure dependence could be done if more experimentally determined entry branching ratios and more concentration profiles were available, which, unfortunately, was not the case.

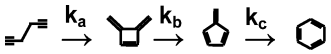

Figure 8. A simple sequential one-route benzene formation model.

2. Implication for C_6H_6 Chemistry. The mechanistic information on benzene formation from the self-reaction of propargyl radicals and from the early isomeric product wells have been the subject of debate for long time. Disputes focused on whether benzene can be formed from other intermediates without involving fulvene. Most experimental work suggested the existence of an additional route forming benzene, as opposed to theoretical calculations performed at various levels of sophistication that suggested that benzene is produced solely via the fulvene → benzene route. Our recent experimental work on 15HD and propargyl recombination[18,30] clearly indicates that benzene is formed by three distinct routes of which only two involve fulvene as a precursor to benzene. In terms of modeling, the difference between the current work and a model that assumes that benzene can only be formed sequentially from fulvene can be clearly demonstrated by considering the mechanism of Thomas et al.[46] shown in Figure 8. It was found that the agreement between the predictions of the Thomas et al. model and the recent HPST data of 15HD thermal rearrangement is poor. Even with the help of the PGN approach, the agreement after optimization with experimental data is still not good, as displayed in Figure 9. The failure is plausible because the Thomas et al. model cannot account for the formation of benzene at relatively low temperatures by the isomerization of 13HD5Y.

Thus the present work has further verified the two-route benzene formation scheme: (a) 13HD5Y → benzene and (b) fulvene → benzene. Reaction pathway analysis on the proposed subdetailed $C_3H_3 + C_3H_3$ model indicated that the relative

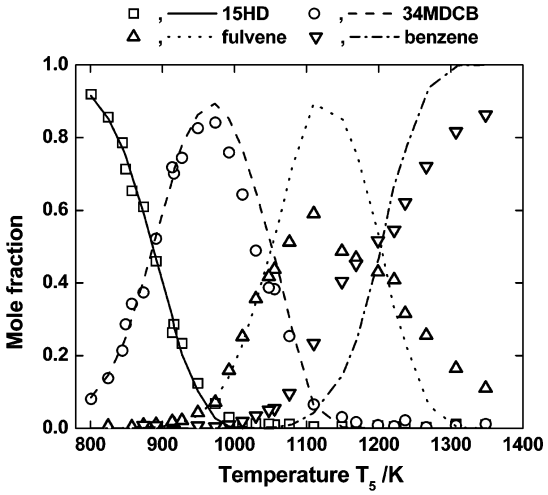

Figure 9. The possible best predictions by using the sequential model in Figure 8 with optimal rate parameters determined by the PGN method. Symbols represent shock tube data of 1,5-hexadiyne isomerization at 25 bar (ref 30). Lines represent predictions using optimized rate parameters.

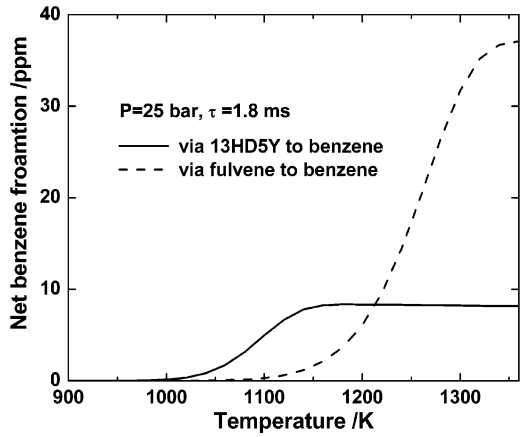

Figure 10. Net formation of benzene contributed by two different routes as a function of temperature. Reaction pathway analysis was performed at 25 bar and 1.8 ms reaction time on a reagent mixture of 100 ppm C_3H_3I in argon.

importance of routes (a) and (b) in contributing to benzene formation is strongly temperature dependent. In the self-reaction of propargyl radicals, the benzene is formed around 1000 K primarily through 13HD5Y and the fulvene to benzene route will not be effective until around 1100 K, Figure 10. The 13HD5Y → benzene route plays the dominant role only above 1200 K, when the two routes contribute to benzene formation equally.

One may easily notice that the proposed model is able to predict extremely well the detailed concentrations of species formed in earlier wells on the PES, specifically 15HD, 34DMCB, 12HD5Y, and 13HD, but shows a small deficiency in simulating species formed in later wells on the PES (benzene and fulvene). This observation is also highlighted in the rate constant comparison diagram, Figure 11. The optimization rate constant results show good agreement with previously recommended rate constants for 34DMCB → fulvene, fulvene → 2E13BD, and 2E13BD → fulvene, but have some discrepancy for fulvene → benzene. Thus it appears that the isomerization between species formed in earlier wells has been understood quite well but not with later ones, particularly the one from fulvene to benzene. However, it is worth pointing out that the obtained Arrhenius parameter values (*A* and *E*) were the result of a mathematical parametrization using the PGN technique and might fail to describe the underlying physical reality, in particular, the preexponential factors for reactions R8−R10 are unrealistically high**.** Here, the optimized k_8-k_{10} represent their high-pressure limits at $T > 1050$ K (cf. sensitivity discussion with Figure 5). Previously, a direct experimental investigation of fulvene to benzene isomerization by Gaynor et al.[47] has generated an Arrhenius rate expression, but the accuracy was questioned by Madden et al.[48] on the basis of their theoretical investigation. They concluded that the activation energy obtained by Gaynor et al. maybe too low. In the present work, the optimized preexponential *A* factor of benzene → fulvene appears to be too high, compared to the value using classical transition-state theory from the vibrational frequencies obtained by Miller and Klippenstein.[24] However, until a better description of the fulvene to benzene isomerization can be obtained, it is premature to force the optimization results to favor the theoretical calculations over the experimentally determined rate coefficient, even though the current model would perform more accurately for the species formed in later wells if the activation energy was increased and the *A* factor was reduced.

3. Implication for Flame Chemistry. Flame modeling shows that, as mentioned before, propargyl recombination is often the dominant route forming benzene. Relatively high mole fraction of propargyl (10^{-3})[25,26] and multiple isomeric C_6H_6 species have been observed in acetylene and ethylene flames.[25−27] Unquestionably, the chemical compositions of the flame structure in terms of C_6H_6 species cannot be reflected by a traditional detailed kinetic model because, in it, the submechanism of propargyl self-reaction is normally represented by only a few global reaction steps and up to two different isomers (benzene and fulvene). In the current work, some existing models were modified by inclusion of the optimized propargyl recombination submechanism in place of the global reactions.

Two aromatic models were considered: (a) the flame model developed by Richter and Howard[9] for prediction of single-ring aromatic hydrocarbons and their precursors in four laminar premixed flames, referred to as model A; and (b) the flame model developed by Rasmussen and co-workers[10] aimed at determining the overall rate constant of the recombination of propargyl radicals at flame conditions (high temperature and low pressure) from the measurements in a fuel-rich premixed acetylene flame, referred to as model B. These two kinetic models have considerable different reaction pathways, but both are capable of simulating accurately their targeted flame structures, species concentration profiles as a function of the burner height. Both models include propargyl recombination as the main step to benzene formation with a single global reaction step but with different products: $C_3H_3 + C_3H_3 \rightarrow$ benzene in model A, and $C_3H_3 + C_3H_3 \rightarrow$ phenyl + H in model B. To maintain the fidelity of original models, only the corresponding single propargyl recombination step was replaced by the semidetailed $C_3H_3 + C_3H_3$ subset in Table 1. To extend the subset to low-pressure premixed flame conditions, rate parameters of dissociation reactions of $k_{11}-k_{14}$ at 30 Torr were taken from ref 24. No further modifications were made to the subset from the optimization procedure or to the original detailed flame models.

Figure 12 presents the isomeric C_6H_6 concentration profiles predicted by model A with the inclusion of the optimized $C_3H_3 + C_3H_3$ subset in a fuel-rich premix ethylene/oxygen/argon flame ($\phi = 1.9$, 50.0% argon, $v = 62.5$ cm·s^{-1}, 20 Torr).[49] The updated model predicts considerable amounts of benzene, fulvene, and 2E13BD. Benzene reaches its highest concentration

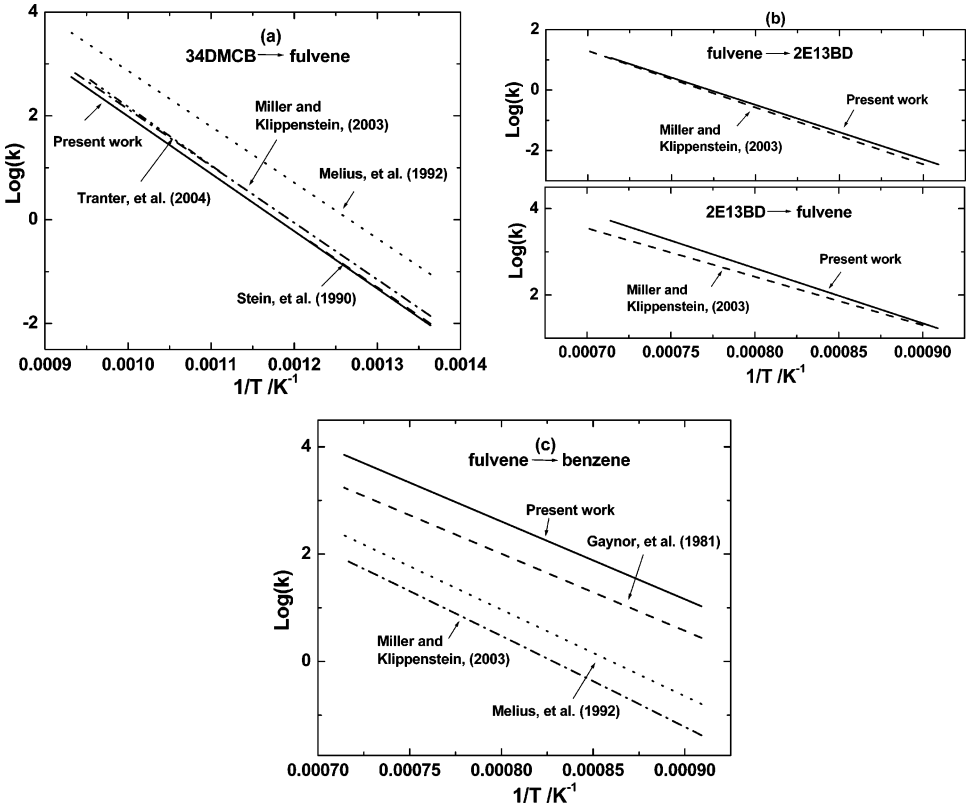

Figure 11. Comparison of Arrhenius plots of (a) 3,4-dimethylenecyclobutene (34DMCB) → fulvene, (b) 2-ethynyl-1,3-butadiene (2E13BD) ↔ fulvene, and (c) fulvene → benzene.

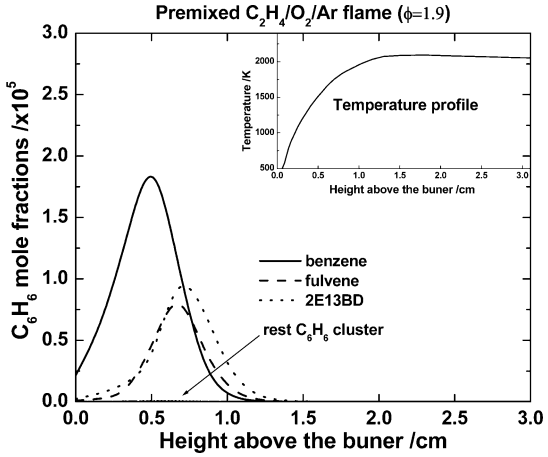

Figure 12. C_6H_6 mole fraction profiles in a fuel-rich ethylene/oxygen/argon flame ($\phi = 1.9$, 50.0% argon, $v = 62.5$ cm·s^{-1}, 20 Torr) predicted by a detailed kinetic model (ref 9) updated by the proposed $C_3H_3 + C_3H_3$ subset. Inset: the figure (up right) is a temperature profile (ref 49). See text for details.

at 0.5 cm above the burner, while the peaks of fulvene and 2E13BD appear with about the same heights but higher than benzene. At their peak locations, the relative ratios are 50% benzene, 23% fulvene, and 27% 2E13BD. Note that no large relative percentages of 15HD were predicted at flame temperature, which is consistent with the shock tube study.[18,30]

The original model A by Richter and Howard was developed against experimental data that did not resolve different C_6H_6 species.[9] Therefore, to study further the consequences of adding our $C_3H_3 + C_3H_3$ submechanism to model A, it was necessary to use the flame measurements of Law et al. that gave relative C_6H_6 ratios. The experimental investigation of a fuel-lean premixed $C_2H_4/O_2/Ar$ flame by Law and co-workers[27] quantitatively specified three different C_6H_6 species (45% benzene, 20% fulvene, and 35% 1,5-hexadiyne) by using molecule-beam mass spectrometry (MBMS) in conjunction with photo-ionization (PIE) measurement and assuming the same cross-sections for all C_6H_6 species. However, one perhaps should be cautious with the assignment of 15HD because both experimental and theoretical work has suggested that 15HD is barely able to survive at temperature >1200 K. The primary point of this comparison is that our proposed compact model can predict multiple C_6H_6 species in flame conditions when the original model A by Richter and Howard does not have such a capability because its $C_3H_3 + C_3H_3$ submechanism only contains benzene and fulvene.

In the other case, the updated model B predicts 60% benzene, 20% fulvene, and 20% 2E13BD in a fuel-rich acetylene flame, Figure 13, a slightly higher percentage of benzene than in the ethylene flame but with the relative ratio of 2E13BD to fulvene remaining the same. Experimental measurements of an acetylene flame by Westmoreland using GC/MS detected the presence of unidentified C_6H_6 isomers eluting before benzene with total concentrations approximately one-fourth that of benzene,[25,26] consistent with the prediction shown in Figure 13. Therefore, the present simulation results suggest that, including our proposed propargyl recombination subset into an aromatic formation model can better predict the flame observations of multiple forms of C_6H_6 species than models that include simplified mechanisms for benzene formation from propargyl.

It should be noted that sensitivity analysis showed that the relative ratios of benzene, fulvene, and 2E13BD are heavily dependent on the initial recombination branching ratios. An even better fit to measured C_6H_6 yields at flame conditions could be obtained by change the branching ratios of propargyl recombination. However, changing the branching ratios is not currently recommended, considering the possible uncertainty in the quantification of flame structure and the authenticity of flame

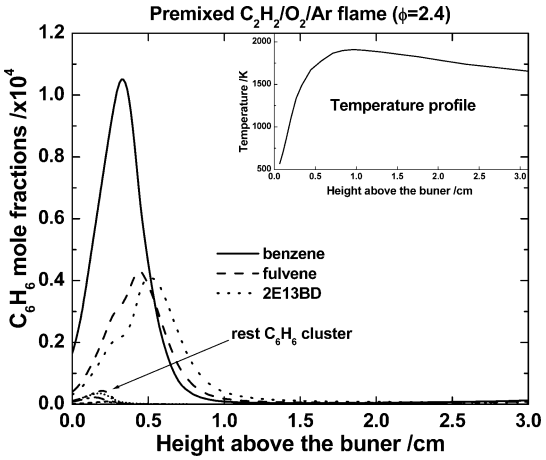

Figure 13. C_6H_6 mole fraction profiles in a fuel-rich acetylene/oxygen/argon flame ($\phi = 2.4$, 5% argon, $v = 50$ cm·s^{-1}, 20 Torr) predicted by a detailed kinetic model (ref 10) updated by the proposed $C_3H_3 + C_3H_3$ subset. Inset: the figure (up right) is experimental temperature profile (refs 25, 26). See text for details.

models in predicting the flux-forming propargyl radicals and the consumption of benzene.

Further application of the current optimized model developed through comparison with experimental data obtained at tens of atmospheres to the simulation of flame data that may have been obtained at a few Torrs bears discussion. Although the proposed $C_3H_3 + C_3H_3$ subset is much more comprehensive than those normally used (i.e., one global step) and is able to predict C_6H_6 species distributions at very high pressures, it is still a simplification of a very complex system that involves multiple channels and multiple wells as cleared mapped out by Miller and Klippenstein.[24] In addition, the underlying approximation upon which the current model was developed that leads to replacing intrinsically pressure-dependent chemically activated reactions with pressure-independent thermally activated reaction steps is not completely realistic. This assumption might be responsible for the model failing to describe the results of the low-pressure experimental studies, in particular the study by Alkemade and Homann[19] at 2.25 Torr and 4.5 Torr in which a large amount of 1245HT and 12HD5Y were observed and no 2E13BD was detected, and two other studies by Shafir et al.[22] and Howe and Fahr,[23] respectively. Consequently, it is advised to limit the model's application to reaction conditions at high pressure in order to ensure quantitative accuracy.

Conclusions

A 14-step semidetailed $C_3H_3 + C_3H_3$ submechanism, including seven isomeric C_6H_6 products is proposed for inclusion into aromatic models to achieve better descriptions of benzene formation from propargyl radicals in flame conditions at high pressures. The subset was constructed based on recent understanding of direct propargyl recombination and subsequent C_6H_6 isomerization and on a rigorous optimization procedure using a novel numeric technique against multiple detailed species profiles. The optimized subset is capable of simulating extremely well all species profiles that were measured in a high-pressure shock tube and an atmospheric flow reactor. Two different detailed flame models with the substitution of the proposed $C_3H_3 + C_3H_3$ subset for the original benzene formation mechanism are able to predict the existence of multiple C_6H_6 isomers.

Acknowledgment. This work was supported by the United States National Science Foundation under contract CTS 0109053. The authors thank Dr. Richter of Massachusetts Institute of Technology and Dr. Glarborg of Technical University of Denmark for kindly providing their flame mechanisms.

Supporting Information Available: The proposed optimized semidetailed $C_3H_3 + C_3H_3$ kinetic model, including thermochemistry and transport properties. This material is available free of charge via the Internet at http://pubs.acs.org.

References and Notes

(1) Miller, J. A. *Faraday Discuss.* **2001**, *119*, 461.
(2) Miller, J. A. *Proc. Combust. Inst.* **1996**, *20*, 461.
(3) Richter, H.; Howard, J. B. *Prog. Energy Combust. Sci.* **2000**, *26*, 565.
(4) Lindstedt, P. *Proc. Combust. Inst.* **1998**, *27*, 269.
(5) Frenklach, M. *Phys. Chem. Chem. Phys.* **2002**, *4*, 2034.
(6) Westmoreland, P. R.; Dean, A. M.; Howard, J. B.; Longwell, J. B. *J. Phys. Chem.* **1989**, *93*, 8171.
(7) D'Anna, A.; Kent, J. *Combust. Flame* **2003**, *132*, 715.
(8) D'Anna, A.; D'Allessio, A.; Kent, J. *Combust. Flame* **2001**, *125*, 1196.
(9) Richter, H.; Howard, J. B. *Phys. Chem. Chem. Phys.* **2002**, *4*, 2034.
(10) Rasmussen, C. L.; Skjøth-Rasmussen, M. S.; Jensen, A. D.; Glarborg, P. *Proc. Combust. Inst.* **2005**, *30*, 1023.
(11) Appel, J.; Bockhorn, H.; Frenklach, M. *Combust. Flame* **2000**, *121*, 122.
(12) Pope, C. J.; Miller, J. A. *Proc. Combust. Inst.* **2000**, *28*, 1519.
(13) Castaldi, M. J.; Marinov, N. M.; Melius, C. F.; Huang, J.; Senkan, S. M.; Pitz, W. J.; Westbrook, C. K. *Proc. Combust. Inst.* **1996**, *26*, 693.
(14) Lindstedt, P.; Skevis, G. *Proc. Combust. Inst.* **1996**, *26*, 693.
(15) Lindstedt, R. P.; Skevis, G. *Combust. Sci. Technol.* **1997**, *125*, 73.
(16) Melius, C. F.; Miller, J. A.; Evleth, E. M. *Proc. Combust. Inst.* **1992**, *24*, 621.
(17) Miller, J. A.; Melius, C. F. *Combust. Flame* **1992**, *91*, 21.
(18) Tang, W.; Tranter, R. S.; Brezinsky, K. *J. Phys. Chem. A*, **2005**, *109*, 6056.
(19) Alkemade, U.; Homann, K. H. *Z. Phys. Chem.* **1989**, *161*, 19.
(20) Fahr, A.; Nayak, A. *Int. J. Chem. Kinet.* **2000**, *32*, 118.
(21) Scherer, S.; Just, T.; Frank, P. *Proc. Combust. Inst.* **2000**, *28*, 1511.
(22) Shafir, E. V.; Slagle, I. R.; Knyazev, V. D. *J. Phys. Chem. A* **2003**, *107*, 8893.
(23) Howe, P. T.; Fahr, A. *J. Phys. Chem. A* **2003**, *107*, 9603.
(24) Miller, J. A.; Klippenstein S. J. *J. Phys. Chem. A* **2003**, *107*, 7783.
(25) Westmoreland, P. R.; Howard, J. B.; Longwell, J. B. *Proc. Combust. Inst.* **1986**, *21*, 773.
(26) Westmoreland, P. R. Ph.D. Thesis, Massachusetts Institute of Technology, Cambridge, MA, 1986.
(27) Law, M. E.; Carriere, T.; Westmoreland, P. R. *Proc. Combust. Inst.* **2005**, *30*, 1433.
(28) Tang, W.; Tranter, R. S.; Brezinsky, K. *Proceedings of the Centre State Meeting of the U. S. Sections of The Combustion Institute,* Austin, Texas, March, 16−18, 2004.
(29) Tang, W.; Zhang, L.; Linninger, A. A.; Tranter, R. S.; Brezinsky, K. *Ind. Eng. Chem. Res.* **2005**, *44*, 3626.
(30) Tranter, R. S.; Tang, W.; Anderson, K. B.; Brezinsky, K *J. Phys. Chem. A* **2004**, *108*, 3406.
(31) Stein, S. E.; Walker, J. A.; Suryan, M.; Fahr, A. *Proc. Combust. Inst.* **1990**, *23*, 85.
(32) Kislov, V. V.; Nguyen, T. L.; Mebel, A. M.; Lin, S. H.; Smith, S. C. *J. Chem. Phys.* **2004**, *120*, 7008.
(33) Kee, R. J.; Rupley, F. M.; Miller, J. A. *Chemkin-II: A Fortran Chemical Kinetics Package for the Analysis of Gas-Phase Chemical Kinetics*; Report SAND 89-8009; Sandia National Laboratories: Albuquerque, NM, 1990.
(34) Burcat, A. Third Millennium Thermodynamic Database for Combustion and Air-Pollution Use. ftp://ftp.technion.ac.il/pub/supported/aetdd/thermodynamics/BURCAT. THR (accessed 2005).
(35) Carstensen, H.-H.; Dean A. M. Private communication.
(36) Fernandes, R. X.; Hippler, H.; Olzmann, M. *Proc. Combust. Inst.* **2005**, *30*, 1033.
(37) Davis, S. G.; Joshi, A. V.; Wang, H.; Egolfopoulos, F. *Proc. Combust. Inst.* **2005**, *30*, 1283.
(38) Eiteneer, B.; Frenklach, M. *Int. J. Chem. Kinet.* **2003**, *35*, 391.
(39) Frenklach, M.; Wang, H.; Rabinowitz, M. J. *Prog. Energy Combust. Sci.* **1992**, *18*, 47.
(40) Frenklach, M.; Packard, A.; Seiler, P.; Feeley, R. *Int. J. Chem. Kinet.* **2004**, *36*, 57.

(41) Lutz, A. E.; Kee, R. J.; Miller, J. A. *SENKIN: A Fortran Program for Predicting Homogeneous Gas-Phase Chemical Kinetics with Sensitivity Analysis*; Report 87-8248; Sandia National Laboratories: Albuquerque, NM, 1988.

(42) Hippler, H.; Luther, K.; Troe, J. *Ber. Bunsen-Ges. Phys. Chem.* **1973**, *77*, 1104.

(43) Kee, R. J.; Rupley, F. M.; Miller, J. A.; Coltrin, M. E.; Grcar, J. F.; Meeks, E.; Moffat, H. K.; Lutz, A. E.; Dixon-Lewis, G.; Smooke, M. D.; Warnatz, J.; Evans, G. H.; Larson, R. S.; Mitchell, R. E.; Petzold, L. R.; Reynolds, W. C.; Caracotsios, M.; Stewart, W. E.; Glarborg, P.; Wang, C.; Adigun, O. *CHEMKIN Collection*, Release 3.6; Reaction Design, Inc.: San Diego, CA, 2001.

(44) Poling, B. E.; Prausnitz, J. M.; O'Connell, J. P. *The Properties of Gases and Liquids*, 5th ed.; McGraw-Hill: New York, 2001.

(45) Joback, K. G.; Reid, R. C. *Chem. Eng. Commun.* **1987**, *57*, 233. Also at http://www.pirika.com/chem/TCPEE/CriP/jobackCP.htm, 2004.

(46) Thomas S. D.; Communal F.; Westmoreland, P. R. *ACS, Div. Fuel Chem.* **1991**, 1449.

(47) Gaynor, B. J.; Gilbert, R. G.; King, K. D.; Harman, P. J. *Aust. J. Chem.* **1981**, *34*, 449.

(48) Madden, L. K.; Mebel, A. M.; Lin, M. C.; Melius, C. F. *J. Phys. Org. Chem.* **1996**, *9*, 801.

(49) Bhargava, A.; Westmoreland, P. R. *Combust. Flame* **1998**, *113*, 333.